Creep Characterization of Type 316LN and HT-9 Stainless Steels by the K-R Creep Damage Model

Woo-Gon Kim*, Sung-Ho Kim, Woo-Seog Ryu
Department of Reactor Core Materials, Korea Atomic Energy Research Institute, Taejon 305-600, Korea

The Kachanov and Rabotnov (K-R) creep damage model was interpreted and applied to type 316LN and HT-9 stainless steels. Seven creep constants of the model, A, B, k, m, λ, r, and q were determined for type 316LN stainless steel. In order to quantify a damage parameter, the cavity was interruptedly traced during creep for measuring cavity area to be reflected into the damage equation. For type 316LN stainless steel, $\lambda=\varepsilon_R/\varepsilon^*$ and $\lambda_f=\varepsilon/\varepsilon_R$ were 3.1 and increased with creep strain. The creep curve with $\lambda=3.1$ depicted well the experimental data to the full lifetime and its damage curve showed a good agreement when $r=24$. However for the HT-9 stainless steel, the values of λ and λ_f were different as $\lambda=6.2$ and $\lambda_f=8.5$, and their K-R creep curves did not agree with the experimental data. This mismatch in the HT-9 steel was due to the ductile fracture by softening of materials rather than the brittle fracture by cavity growth. The differences of the values in the above steels were attributed to creep ductilities at the secondary and the tertiary creep stages.

Key Words : Creep Behavior, Damage Parameter, Type 316LN Stainless Steel, HT-9 Stainless Steel, Kachanov-Rabotnov (K-R) Creep Damage Model, Monkman-Grant (M-G) Strain.

1. Introduction

Due to their creep resistance, austenitic stainless steels are materials used for the reactor internals and piping in light water reactors (LWR) and candidate materials for the structural components in liquid metal reactors (LMR). Besides, 9-12%Cr martensitic stainless steels are prospective materials for the nuclear fuel cladding tube, nozzle and flow piping in LMR because of higher thermal fatigue strength and lower swelling resistance than austenitic stainless steels (Oh and Hong, 2000 ; Ryu et al., 1998 ; Kim et al., 2000).

* Corresponding Author,
E-mail : wgkim@kaeri.re.kr
TEL : +82-42-868-2493; **FAX** : +82-42-868-8549
Senior Researcher, Department of Reactor Core Materials, Korea Atomic Energy Research Institute, P. O. Box 105, Yusong, Taejon 305-600, Korea.(Manuscript **Received** November 17, 2000 ; **Revised** August 17, 2001)

Since these structural components in nuclear power plants are operated at elevated temperatures, the most critical factor in determining the integrity of their components is creep behavior. Creeping components are therefore designed through the criteria of acceptable permanent deformation, allowable stress, and specified lifetime by fracture. However, the components are generally hard to meet the design criteria due to complicated interactions between sustained loads and temperatures, change in stress patterns in redundant structures, and thermal-chemical instabilities (Viswanathan, 1989 ; Belloni and Bernasconi, 1978 ; Kim and Lee, 1996). In order to properly design and analyze the structures, it is necessary to know not only the constitutive law relating to the interconnections between stress, strain, time, and temperature, but also the damage law relating to the damage effects of cracks and voids in the materials.

A constitutive model of a material relates the

creep strain rate to the measurable parameters of load, stress, strain, time and temperature. In addition, internal variables (ω_1, ω_2, $\cdots$), which cannot be measured directly are included as

$$\frac{d\varepsilon}{dt}=f(\sigma,\ \varepsilon,\ t,\ T,\ \omega_1,\ \omega_2,\ \cdots). \tag{1}$$

In addition to this equation, Eg(2) is also reguired to, describ ω as

$$\frac{d\omega}{dt}=f_1(\sigma,\ \varepsilon,\ t,\ T,\ \omega_1,\ \omega_2,\ \cdots). \tag{2}$$

Any of the external or internal variables, σ, ε, t, T, ω_1, ω_2, can be used as a damage counter or parameter (Leckie and Hayhurst, 1975, 1977; Penny and Marriott, 1995; Kim et al., 2001).

As far as creep damage is concerned, the work of Kachanov and Rabotnov (K-R) is well known to predict rupture and static strength deterioration. It was originally postulated by Kachanov that damage occurred during the secondary creep will progressively reduce continuity of the cross-section of a specimen from an initially intact condition to the complete loss at rupture occurrence. Prediction of damage for the loss of continuity can be made by equations which accomimodate these limiting conditions (Kachanov, 1958, 1986; Rabotnov, 1969). A study by Penny (1974) reported a damage model which showed a reasonable agreement in an aluminum alloy. Also, Dyson and McLean (1972), Cane and Greenwood (1975), Brathe (1978), and Belloni et al. (1977) presented the expected form by measuring the cavity density for Nimonic 80A alloy or low-alloy bainitic steels. However, the practical usefulness of the K-R model of creep damage for type 316LN stainless steel (hereafter, 316LN) and 12Cr-1Mo martensitic stainless steel (hereafter HT-9) has not been demonstrated by others.

The purpose of this work is to provide the creep constants necessary to use the K-R damage equations : the systematic analysis procedure will be followed, and then the equations will be applied to the 316LN and the HT-9 steels. As a result the K-R creep curves of the two steels and will be presented and discussed a damage parameter for the 316LN steel.

2. Interpretation of Damage Equations

Kachanov (1958) proposed a theory of brittle rupture based on the concept of what he called the continuity, ω, of a material ; damage accumulation changes the proportion of the material available to carry the load as time passes. Under the constant load, the average stress increases according to the amount of damage until continuity is destroyed and eventually rupture occurs.

On a specimen of an initial cross section area, A_0, subjected to a load P the initial stress is $\sigma_o=P/A_o$. At a time t at which the specimen is damaged, the cross sectional area A_t is reduced as

$$A_t=A_0(1-\omega) \tag{3}$$

and the stress σ_t at time t is

$$\sigma_t=\sigma_o\frac{A_o}{A_t}=\frac{\sigma_o}{(1-\omega)} \tag{4}$$

In these equations, $(1-\omega)$ can be regarded as the loss of cross-section area. To calculate the variation of damage with time, Kachanov assumed a power-law relationship between the continuity and stress as

$$\frac{d\omega}{dt}=K\sigma_t^{\nu} \tag{5}$$

where constants, k and υ, are determined through experiment. Substituting Eq.(4) into Eq.(5), we obtain

$$\frac{d\omega}{dt}=K\sigma_o^{\nu}(1-\omega)^{-\nu} \tag{6}$$

In the case of initially damage-free material, Eq.(6) can be integrated with the conditions $\omega=0$ at $t=0$ and $\omega=1$ at $t=t_R$, where a complete continuity is assumed at zero time and the complete loss of continuity at rupture, to give Eq.(7) as

$$\int_0^1(1-\omega)^{\nu}d\omega=\int_0^{t_R}K\sigma_0^{\nu}dt$$

$$t_R=\frac{1}{K(1+\nu)\sigma_0^{\nu}} \tag{7}$$

The log σ−log t plot for Eq.(7) is usually used.

Later, Rabotnov (1969) generalized these concepts to predict creep strain accumulation as

well as of rupture time, assuming that the primary creep is negligible. As in Kachanov's approach, $\omega=0$ corresponds to the condition of undamaged material and $\omega=1$ to the formation of macroscopic cracks. Here, ω is the only structural parameter which defines a state of cracking, so that if initial elastic and plastic strains are neglected, then the creep strain and damage can be defined by

$$\frac{d\varepsilon}{dt}=f_1(\sigma,\ \omega)\ \text{ and }\ \frac{d\omega}{dt}=f_2(\sigma,\ \omega) \tag{8}$$

Eq. (8) depend on the stress level in relation to the yield stress and the stress σ may be referred as either engineering stress or true stress. If the deformations are small, ε is taken as the engineering strain, and if large, as the logarithmic strain.

The functions f_1 and f_2 are taken as power functions of the form

$$\frac{d\varepsilon}{dt}=A\sigma^m(1-\omega)^{-q}=\frac{\dot{\varepsilon}_o}{(1-\omega)^q} \tag{9}$$

$$\frac{d\omega}{dt}=B\sigma^k(1-\omega)^{-r}=\frac{\dot{\omega}_o}{(1-\omega)^r} \tag{10}$$

where A and B are temperature dependent. For practical cases of a low stress region, failure deformations may be considered small, so that, brittle rupture occurs. Putting $\sigma=\sigma_o$, and integrating of Eqs. (9) and (10), their solution gives in the following expressions, subject to the conditions $\omega=0$ at $t=0$ and $\omega=1$ at $t=t_R$,

$$(1-\omega)^{1+r}=1-B(1+r)\sigma_o^k t \tag{11}$$

$$\varepsilon=\frac{\lambda A}{B(1+r)}\cdot\sigma_o^{m-k}\{1-[1-B(1+r)\sigma_o^k t]^{1/\lambda}\} \tag{12}$$

$$\varepsilon_R=\frac{\lambda}{(1+r)}\cdot\frac{A}{B}\cdot\sigma^{m-k} \tag{13}$$

$$t_R=\frac{1}{B(1+r)\sigma_o^k} \tag{14}$$

$$\varepsilon_R=\lambda\varepsilon^*\ (\varepsilon^*=\dot{\varepsilon}_o t_R=A\sigma_o^m t_R) \tag{15}$$

$$\lambda=\frac{1+r}{1+r-q} \tag{16}$$

where ε_R is the strain at rupture, ε^* is the Monkman-Grant (M-G) strain (Penny and Marriott, 1995), and σ_0 is the initial stress at constant load test. Rearranging in terms of the life fraction, t/t_R, the local damage and strain values become

$$(1-\omega)^{1+1}=1-\frac{t}{t_R} \tag{17}$$

$$\varepsilon=\varepsilon_R\left[1-\left(1-\frac{t}{t_R}\right)^{1/\lambda}\right]=\varepsilon^*\lambda\left[1-\left(1-\frac{t}{t_R}\right)^{1/\lambda}\right] \tag{18}$$

$$\text{where }\ \varepsilon_R=\frac{A\sigma_o^m}{\left(1-\frac{q}{1+r}\right)}\cdot\ t_R=\frac{\varepsilon^*}{\left(1-\frac{q}{1+r}\right)} \tag{19}$$

3. Experimental Procedures

Laboratory ingots of 316LN and HT-9 alloys were prepared by the vacuum induction melting (VIM) and their chemical compositions are shown in Table 1. The ingots were annealed at 1150℃ for 2 hr at an argon atmosphere and reduced to 15 mm by the hot rolling process. For heat treatment, the 316LN was solution annealed at 1100℃ for 1 hr and water quenched. HT-9 was treated by normalizing and tempering. Normalizing was held at 1050℃ for 1 hr and followed by air cooling and then tempering at 750℃ for 2 hr and finally air cooled. Creep specimens were taken as the rolling direction and machined to be cylindrical with a 30 mm gage length and 6 mm diameter. The gage sections of specimens were polished using 1000 grit sand paper with strokes along the specimen axis. Creep tests were carried out using constant load machines with the 20/1 lever ratio. The test temperature was maintained constantly within ±2℃ during the period of the test. All specimens were held at the test temperature for 1 hr before starting the test. All creep data were automatically acquired through a personal computer. A number of creep tests were accomplished under different stress and temperature conditions for 316LN and HT-9 steels.

Table 1 Chemical compositions of type 316LN and HT-9 stainless steel (wt.%)

Specimens	Fe	C	Si	Mn	P	S	Cr	Ni	Mo	N	Nb	W	V
316LN	bal.	0.019	0.63	0.97	0.018	0.004	17.26	12.35	2.41	0.10	-	-	-
HT-9	bal.	0.190	0.10	0.59	0.019	0.004	11.79	0.53	0.99	0.01	0.02	0.45	0.31

Table 2 The λ and ε^* values determined from experimental data for type 316LN and HT-9 stainless steels

Materials & Conditions		$t_R(hr)$	$\dot{\varepsilon}_0(sec^{-1})$	$\varepsilon_R(\%)$	$\varepsilon^*(\%)$	$\lambda(=\varepsilon_R/\varepsilon^*)$		λ_f
316LN steel	550℃/320MPa	591.4	4.15E-8	31.3	8.86	3.5	3.1 (Avg.)	3.1 Value fitted by $\varepsilon/\varepsilon_R$
	550℃/300MPa	1679.8	1.48E-8	28.8	8.94	3.2		
	550℃/290MPa	3321.4	6.57E-9	23.3	7.85	3.0		
	620℃/260MPa	457.2	8.40E-8	38.4	13.80	2.8		
HT-9 steel	600℃/200MPa	320.8	3.41E-9	24.3	3.93	6.2	6.2 (Avg.)	8.5 Value fitted by $\varepsilon/\varepsilon_R$
	600℃/190MPa	1143.5	9.7E-9	23.2	3.77	6.2		
	650℃/130MPa	261.1	3.78E-8	22.8	3.55	6.4		
	650℃/125MPa	585.4	1.57E-8	20.8	3.32	6.3		
	650℃/120MPa	852.4	1.08E-8	20.3	3.31	6.1		

In addition, for characterizing creep damage, creep cavity is regarded as a damage parameter which stands out the real material behavior because it captures a large portion of the creep deformation and damage accumulation as time passes. So, its amount was quantified by measuring from intentionally interrupted creep tests at 20 hrs, 130 hrs, 327 hrs, 430 hrs, and 457 hrs (rupture) under 620℃ and 260 MPa for 316LN specimen. It has been expected to quantify creep damage effect with time variation from interrupting test because creep cavity could reflect material behavior during creep. The creep cavity has been commonly regarded as a reasonable variable to find creep damage effect in a high temperature material.

After testing, every specimen was cooled by gas quenching and a small sample was taken at the center part of the gage length. Electro polishing followed for 5~10 seconds under 19 voltage in a mixed solution of 80% $HClO_4$ (perchloric acid) and 20% CH_3COOH (acetic acid). Finally, the crept cavities were examined using scanning electro microscopy (JEOL, JSM-5200).

4. Results and Discussion

4.1 Creep strain curves

Figure 1 shows the results of strain fraction ($\varepsilon/\varepsilon_R$) and life fraction($t/t_R$) obtained at different stresses and temperatures for 316LN and HT-9 steels. Symbol marks are the measured data and the solid lines are the curves calculated by Eq.

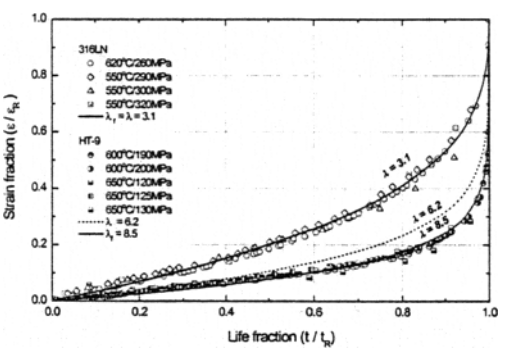

Fig. 1 Strain fraction($\varepsilon/\varepsilon_R$) vs. life fraction($t/t_R$) under different stresses and temperatures for type 316LN and HT-9 stainless steels

(18) where ε_R is the rupture elongation and t_R is the rupture time. All the measured data showed material dependance even though the applied stresses and temperatures were different. λ value was determined by best fitting through Eq. (18) from the measured data. λ was determined as 3.1 for 316LN steel and 8.5 for HT-9 steel.

Table 2 lists the results of λ and ε^*. t_R, $\dot{\varepsilon}_o$ and ε_R are the results obtained by experiment. Hence, ε^* represents the M-G strain of Eq. (15), ε_R/λ, and λ_f represents the experimental value fitted by $\varepsilon/\varepsilon_R$. In type 316LN stainless steel, $\lambda=\varepsilon_R/\varepsilon^*$ and $\lambda_f=\varepsilon/\varepsilon_R$ were almost identical as 3.1. But, in HT-9 stainless steel, λ and λ_f were found to be different as $\lambda=6.2$ and $\lambda_f=8.5$. The λ and ε^* values were different in different steels, but the same materials showed almost similar values regardless of testing conditions. These constants imply clearly a regular tendency of material

dependance. Therefore, these constants may be utilized to predict the lifetime of creeping components.

Figures 2 and 3 show the results of the normalized strain fraction($\varepsilon/\varepsilon^*$) and the life fraction (t/t_R) at different stress and temperature conditions for 316LN and HT-9 steels. In 316LN steel, as shown in Fig. 2, the master curve based on Eq. (18) coincided well with the experimental one regardless of testing stress and temperature conditions. λ and λ_f values were almost identical as 3.1. Thus, this ensures reasonable agreement of the K-R model for type 316LN stainless steel. In regards of HT-9 steel, as shown in Fig. 3, when using the values of λ=6.2 calculated by $\lambda=\varepsilon_R/\varepsilon^*$ or λ_f=8.5 fitted by $\varepsilon/\varepsilon_R$, the curves of the K-R, Eq. (18), did not match the experimental one and over-estimated. Two solid lines in Fig. 3 represent the results calculated by the K-R Eq. (18). They almost coincided in despite of some gaps as λ=6.2 and λ_f=8.5. The experimental data approximately agreed with the curve of $\lambda\approx2$, but the curve did not match the experimental data by 80 percent of the life fraction.

These results in two steels were illustrated by the fracture mode as given in Figs. 4 and 5. The fracture mode of 316LN steel was very different from that of HT-9 steel, as can be seen in (a), (b), and (c) of Figs. 4 (316LN) and 5 (HT-9). Here, the creep failure in 316LN steel showed the domination of intergranular brittle failures ; the fracture path was along grains and grain boundaries, and the failure was initiated by

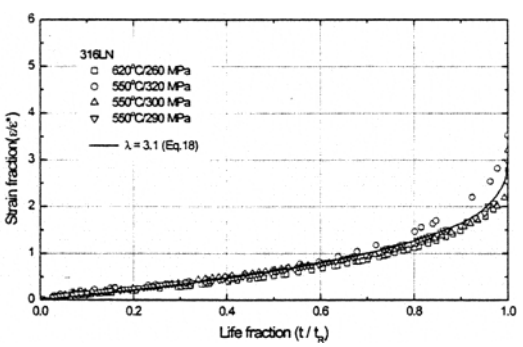

Fig. 2 Normalized strain fraction($\varepsilon/\varepsilon^*$) vs. life fraction($t/t_R$) under different stresses and temperatures for type 316LN stainless steels

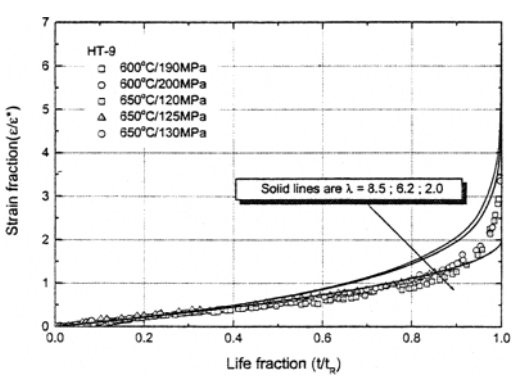

Fig. 3 Normalized strain fraction($\varepsilon/\varepsilon^*$) vs. life fraction($t/t_R$) under different stresses and temperatures for the HT-9 stainless steels

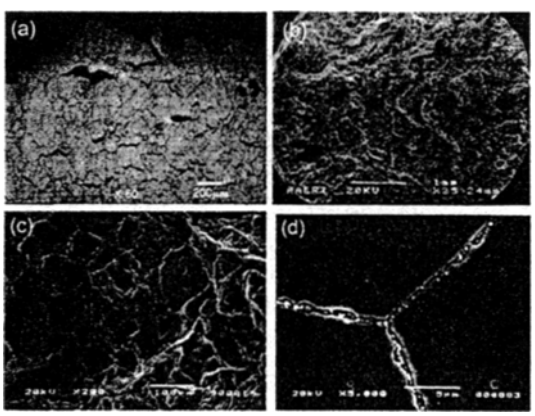

Fig. 4 Plot of the strain rate fraction with life fraction

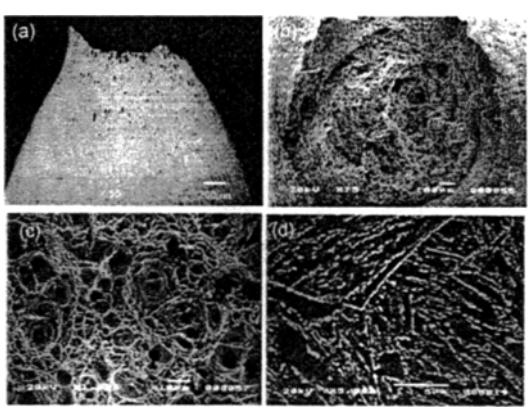

Fig. 5 Cavity area fraction during creep at 620℃ and 260 MPa for type 316LN stainless steel

growth and coalescence of voids in grain boundaries. Voids were widely distributed into the crept specimen. On the contrary, the failure of HT-9 steel showed the domination of the ductile fracture caused by softening of materials. Voids were small and localized at the center of the neck of the fractured specimen. Typical cup-and-cone fracture was observed in the fracture surface, as seen in Fig. 5 (a), (b), and (c). Also, the deformed voids in HT-9 steel were elongated along the load direction, but those in 316LN steel were perpendicular to the load direction. As well, as seen in Figs. 4 (d) and 5 (d), the precipitates formed in the crept specimens of two materials were significantly different. Accordingly, this result in the HT-9 steel was because creep failure showed ductile fracture caused by material softening.

This result shows that the λ values of the two steels are subjected to large differences in rupture elongation or creep rate, because the M-G strain ($\varepsilon^* = t_R \dot{\varepsilon}_o$) in HT-9 steel is lower than that of 316LN steel. Thus, λ is considered to be a sensible constant for determining the shape of the creep curves, and was affected by the rupture strain or the M-G strain.

Figure 6 shows the relationship of $\dot{\varepsilon}_c/\dot{\varepsilon}_o$ expressed in terms of the life fraction and parameter λ, calculated by Eq. (20). It may be derived by differentiating Eq. (18).

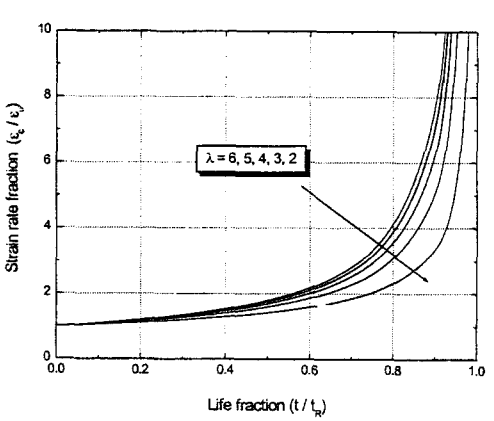

Fig. 6 Cavity growth during an interrupted creep test at 620℃ and 260 MPa for type 316LN stainless steel

$$\frac{\dot{\varepsilon}_c}{\dot{\varepsilon}_o} = \frac{1}{\left(1-\frac{t}{t_R}\right)^{(\lambda-1/\lambda)}} \tag{20}$$

As expected in Fig. 6, the strain rate fraction gives same robustness as the presentation of the creep strain fraction which is shown for type 316LN stainless steel of Fig. 2. The creep strain rate in Fig. 6 is abruptly increased after 80 percent of the lifetime which has almost been consumed. This usefulness of this measure of the progress of creep deformation is that one can use strain rate acceleration as a guide to impending failure. Thus, the strain rate derived from Eq. (20) can be used as another choice of failure criteria. Such trends are easily detectable in most practical applications, and the data of strain rate measures can be represented by Eq. (20).

4.2 Damage curves

The results of the Rabotnov approach to a brittle rupture given in Eq. (17) can be graphically represented. It is necessary to measure the continuous damage during creep for the use of Eq. (17). For this purpose, the cavity amount, which is regarded as creep damage, was measured by interrupted creep tests of five steps at varying times, then the measured cavities were reflected in the damage equation of Eq. (17).

Figure 7 shows the results of the cavity areal fraction (A_c/A_T) and life fraction under 620℃ and 260 MPa for the 316LN specimens. Cavities were formed with a small amount at the secondary creep stage, but the cavities at the tertiary creep stage from 300 hrs to rupture increased abruptly in number and size. SEM photographs of cavity growth with time accumulation are shown in Fig. 8. The cavity size was observed below 200 μm^2 by 300 hrs and 400 μm^2 by 430 hrs (24% strain). Furthermore, some cavities above 800 μm^2 were observed in the ruptured specimens. These large cavities directly affect material deterioration. The growth and coalescence of these cavities are closely associated with total rupture elongation. Substituting to Eq. (17) from the measured cavities, the creep master curve can be obtained.

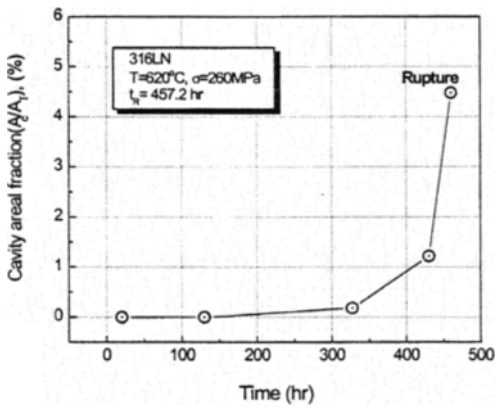

Fig. 7 Cavity areal fraction during creep at 620℃ and 260 MPa for type 316LN stainless steel

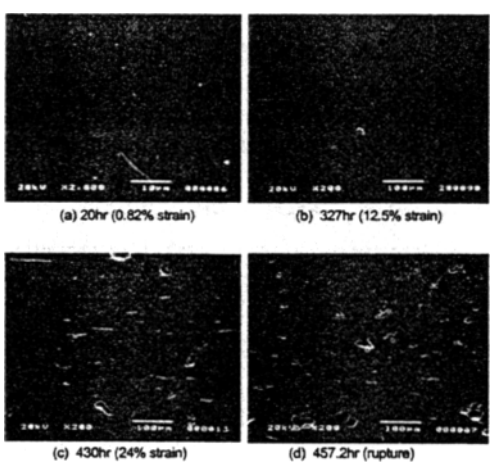

Fig. 8 Cavity growth during an interrupted creep test at 620℃ and 260 MPa for type 316LN stainless steel

Figure 9 shows the damage factor, ω, expressed in terms of the life fraction t/t_R and the exponent r for 316LN steel. The form of damage curve is somewhat similar to the results of cavity density, as shown in Fig. 8. The damage factor decreases with increasing parameter r. The damage curve coincided well at $r=24$, but poorly in the last twenty percent of the lifetime. However, after the last twenty percent of the full lifetime, it would be not important because the creep damage has been almost propagated to failure. Therefore, the parameter r is considened as 24. Using Eq. (16) from the λ and r results, parameter q is also calculated as 16.6. The values of q and r obtained

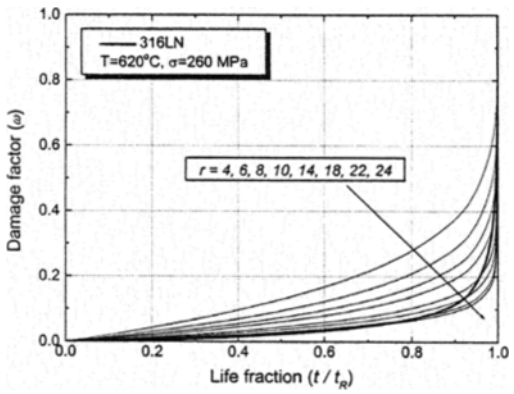

Fig. 9 Variation of damage factor(ω) with life fraction(t/t_R) for type 316LN stainless steel

in 316LN steel are higher than those of 304 stainless steel or other alloys. This result of 316LN steel is believed to be due to high temperature strength increases contributed to a solid-solution strengthening effect from nitrogen addition.

4.3 Determination of creep constants

Seven constants used in the K-R constitutive equations are A, B, k, m, λ, r, and q, where k and m are the stress exponents, q and r the exponents relating to the damage parameter, and A and B the constants, which depend on temperature and material. Also, λ is related to exponents q and r and has important meaning for creep tolerance. If the λ value decreases, the creep resistance of the materials increases, but the q or r values decrease inversely. Many creep data are needed to determine the constants A, B, k and m. The constants A and m can be obtained from the initial strain accumulation data, while k and the product $B(1+r)$ are derived from the rupture data. That is, m can be determined from the slope of $\log\sigma-\log\dot{\varepsilon}$ and k the slope of $\log\sigma-\log t_R$. A and B can then be obtained by calculating Eqs. (8) and (9), respectively.

As stated above, four constants, A, B, k, m, for 316LN steel were determined using the laboratory creep data produced at KAERI (Kim et al., 1998, 2000). The three constants λ, r and q have already been obtained, as described in sections 4. 1 and 4.2. A summary of the seven constants is

Table 3 Constants obtained for type 316LN stainless steel

A ($MPa^{-1}sec^{-1}$)	B ($MPa^{-1}sec^{-1}$)	m	k	λ	q	r
1.980×10^{-25}	4.476×10^{-30}	7.3	9.0	3.3	16.6	24

given in Table 3. The results in Table 3 were obtained at 620℃ of type 316LN stainless steel. In the case of 650℃ of commercial 316 stainless steel, Frost and Ashby (Riedel, 1987) reported that A was 1.60×10^{-27} (MPa^{-1} sec^{-1}) and m was 7.9, and for the 304 stainless steel that A was 1.9×10^{-23} (MPa^{-1} sec^{-1}) and m was 7.0. Comparing these data, the 316LN steel has a gap for the constants of the 304 or 316 stainless steels. It seems that the gap is contributed to the nitrogen-addition effect, temperature gap, chemical compositions.

5. Conclusions

Creep damage for type 316LN and HT-9 stainless steels was examined using the K-R creep damage model. Seven creep constants used in the K-R equations (A, B, k, m, λ, r, and q) were determined for type 316LN stainless steel. For type 316LN stainless steel, both values of $\lambda=\varepsilon_R/\varepsilon^*$ and $\lambda_f=\varepsilon/\varepsilon_R$ were 3.1 and its K-R creep curve agreed well with the experiment to the full lifetime. Damage curve between the damage parameter and life fraction showed a good agreement when $r=24$. On the other hand, for HT-9 stainless steel, $\lambda=\varepsilon_R/\varepsilon^*$ and $\lambda_f=\varepsilon/\varepsilon_R$ were different as $\lambda=6.2$ and $\lambda_f=8.5$. Their K-R creep curves did not match well the experimental data, but approximately coincided with the experimental ones at $\lambda\approx2$. This mismatch in HT-9 steel was because creep failure showed ductile fracture caused by softening of materials. The differences in the λ values on the two steels were attributed to creep ductilities at the secondary and the tertiary creep stages. It is thought that the creep constants obtained for type 316LN stainless steel may be useful to predict the remaining life of creeping components.

Acknowledgements

This work was performed under the Long-term Nuclear R&D Program sponsored by the Korean Ministry of Science and Technology.

References

Belloni, G. , and Bernasconi, G., 1978, "Creep Damage Models," *Creep of Engineering Materials and Structures, Edited by Bernasconi G. and Piatti G., Applied Science Publisher LTD*, London, pp. 195~227.

Belloni, G., Bernasconi, G., and Piatti, G., 1977, "Creep Damage and Rupture in AISI 310 Austenitic Steel", *Meccanica*, Vol. 12, pp. 84~96.

Brathe, L., 1978, "Macroscopic Measurements of Creep Damage in Metals," *Scand. J. Metallurgy*, Vol. 7, pp. 199~203.

Cane, B. J., and Greenwood G. W., 1975, "The Nucleation and Growth of Cavities in Iron during Deformation at Elevated Temperatures," *Metal Sci.*, Vol. 9. pp. 50~60.

Dyson, B. F. and McLean, D., 1972, "A New Method of Predicting Creep Life," *Metal Science Journal*, Vol. 6, pp. 220~223.

Kachanov, L. M., 1958, "On Creep Rupture Time", *Izv. ANSSSR, OTN*, No. 8., pp. 26~31.

Kachanov, L. M., 1986, Introduction to Continuum Damage Mechanics, *Martinus Nijhoff Publishers*, Dordrecht, pp. 1~10.

Kim, W. G., Kim, D. W., and Ryu, W. S., 2000, "Applicability of Monkman-Grant Relationships to Type 316L(N) Stainless Steel", *Transactions of the KSME(A)*, Vol. 24, No. 9, pp. 2326~2333.

Kim, W. G., Kim, D. W., Ryu, W. S., and Kuk I. H., 1998, "Effect of Phosphorus on the Creep Properties in AISI 316L(N) Stainless Steel", *Proc. of the Korean Nuclear Society Autumn Meeting*, Seoul, pp. 216~221.

Kim, W. G., Kim D. W, and Ryu, W. S., 2001, "Creep Design of Type 316LN Stainless Steel by K-R Damage Model", *Transactions of the KSME(A)*, Vol. 24, No. 2, pp. 296~303.

Kim, K. Y., and Lee, K. Y., 1996, "The Life

Assesment of Creep Damaged Components Used High Pressure and Temperature Condition by Metallographic Replicas", *Proc. of Materials and Fracture Part of the KSME 96MF14*, Seoul, pp. 90~96.

Leckie, F. A., and Hayhurst, D. R., 1975, "The Damage Concept in Creep Mechanics", Mech. Res. Comm., Pergamon Press., Vol. 2, pp. 23~26

Leckie, F. A., and Hayhurst, D. R., 1977, "Constitutive Equations for Creep Rupture", *Acta Metallurgical*, Vol. 25, pp. 1059~1070.

Oh, Y. J., and Hong, J. H., 2000, "Nitrogen Effect on Precipitation and Sensitization in Cold -Worked Type 316L(N) Stainless Steels", *Journal of Nuclear Materials*, Vol. 278, pp. 242~250.

Penny, R. K., 1974, "The Usefulness of Engineering Damage Parameters During Creep", *Metal and Materials*, Vol. 8. pp. 278~282.

Penny, R. K., and Marriott, D. L., 1995, Design for Creep, Chapman & Hall, London, pp. 165 ~174.

Rabotnov, Y. N., 1969, Creep in Structural Members, *John Wiley & Sons*, New York, pp. 359~382.

Riedel, H., 1987, Fracture at High Temperature, *Springer-Verlag Berlin*, Heidelberg, p. 390.

Ryu, W. S., Kim, W. G., Kim, D. W., Kuk, I. H., Kim, S. H., Jang, J. S., Rhee, C. K., Chung, M. G., Park, S. D., and Han, C. H., 1998, "A State of the Art Report on LMR Structural Materials", *KAERI/AR-487/98*, pp. 37~47.

Viswanathan, R., 1989, Damage Mechanisms and Life Assessment of High-Temperature Components, *ASM International, Carnes Publication Services*, Inc. Ohio, pp. 10~15.